Role of deformation in exotic decay studies

G. Shanmugam and B. Kamalaharan
Department of Physics, Presidency College, Madras 600 005, India
(Received 4 January 1989; revised manuscript received 28 August 1989)

We have recently constructed a model for exotic decay studies using a cubic potential for the overlapping region that is smoothly connected by a Yukawa-plus-exponential potential for the region after separation. In this model, the zero-point vibration energy is explicitly used without violating the energy conservation and the inertial mass coefficient is made dependent on the center of mass distance, but the deformation effect has not been included. In this work, it is taken into account in both the parent and the daughter nuclei, keeping the emitted nucleus always spherical. This model is applied to the cases of ^{14}C and ^{24}Ne emissions and also for the recently reported cases of ^{26}Ne, ^{28,30}Mg, and ^{34}Si emissions. It is found that the effect of the fragment deformation (which is always very small in the above decays) on lifetime is negligible while the parent deformation plays an appreciable role in the lifetime calculations.

I. INTRODUCTION

The spontaneous emission of fragments heavier than alpha particles, termed as exotic decay, has now become an experimentally confirmed reality. Theoretically, such emissions were first predicted by Sandulescu, Poenaru, and Greiner.[1] The first experimental observation of radioactive decay of heavy nuclei by the emission of a nucleus heavier than alpha particles was made by Rose and Jones[2] from the University of Oxford who reported the radioactive decay of ^{223}Ra by ^{14}C emission with a half-life of $T_{1/2}=(3.7\pm1.1)\times10^7$ years. This result was soon after confirmed by Gales *et al.*[3] and Price *et al.*[4] Encouraged by this, researchers tried to detect other novel modes of radioactive decay in which heavy nuclei disintegrate by emission of intermediate mass fragments. The emission of ^{26}Ne, ^{28,30}Mg, and ^{34}Si from uranic and transuranic nuclei have recently been reported.[5] Theoretically, the interest in such decays lies in the estimation of lifetimes and branching ratios with respect to alpha decay which can be checked with the experimental results. Study of such exotic decay systematics might improve our knowledge regarding nuclear clustering, internucleus potentials, and the nature of asymmetric fission process in nuclei.

Poenaru *et al.*[6] have given a theoretical superasymmetric fission model for exotic decay studies. Even though it has the great advantage of being analytical, still it suffers from the disadvantage that the zero-point vibration energy has been treated as an adjustable parameter to compensate for the overestimation of the barrier height which in turn leads to violation of conservation of energy. An elegant alternate model has been put forth by Shi and Swiatecki[7] by using a proximity-plus-Coulomb potential for the postscission region which brings the barrier heights closer to the experimental values. But this model contains the undesirable arbitrariness of the power of the potential used in the prescission region. Apart from these two major models, there are other models given by Pik-Pichak,[8] de Carvalho *et al.*,[9] and Blendowske *et al.*[10]

In our earlier work,[11] we tried to construct a new model for exotic decay studies free of the defects which may be present in the other available models. This model, which we call the cubic-plus-Yukawa-plus-exponential potential model (CYEM), has a cubic potential for the overlapping region which is smoothly connected by a Yukawa-plus-exponential potential for the region after separation. In this model, the zero-point vibration energy is explicitly included without violating the conservation of energy and the inertial mass coefficient dependent on the center of mass distance has been used. We have already demonstrated the success of this model by applying it to the cases of ^{14}C and ^{24}Ne emissions. We have extended[12] this model for the recently reported emissions of fragments heavier than ^{24}Ne from uranic and transuranic nuclei. But, in all these cases we have used only the two-sphere parametrization and have not taken the deformations of the parent and the fragments into account.

Pik-Pichak[8] studied the deformation effects in his model treating the parent and daughter nuclei in their ground states as spheroids and assuming the light nucleus always as sphere. He assumed that, after scission, only the Coulomb forces act between the fragments and the potential energy is given by the interaction of a uniformly charged sphere and a spheroid. In his model, the finite range effects or the proximity effects were not considered. Shi and Swiatecki[7] first constructed the proximity-plus-Coulomb potential model treating the parent and the fragments as spheres. Later, they[13] estimated the influence of nuclear deformations on the lifetimes of exotic radioactivities. In their study, the emitted fragment was still considered spherical, but the parent and/or daughter might have an axially symmetric deformation. Further, they stated that they have considered the effects of ground-state deformations only.

The aim of this work is to improve our earlier model by including such deformations both in the Coulomb energy and the surface energy due to finite range effects and study their effects on the lifetime calculations in the exotic radioactivities. We have thus modified our earlier model[11] by incorporating the deformations both in the parent and the daughter nuclei keeping the emitted nucleus spherical.

In Sec. II, we present the details of our model incorporating the deformation effects. In Sec. III, we apply the present model to calculate the lifetimes of ^{14}C, ^{24}Ne, and still heavier fragment emissions, and discuss the results obtained.

II. DETAILS OF OUR MODEL

A. Inclusion of deformation effects in the potential for postscission region

In our earlier work, we presented a model[11] for exotic decay studies that essentially consists of a cubic potential in the overlapping region which is smoothly connected by a Yukawa-plus-exponential potential in the region after separation. In this model, the parent and the fragments are treated as spheres. If the daughter nucleus has a deformation, say quadrupole deformation only, while the emitted nucleus is spherical and if the Q value of the reaction is taken as the origin, then the potential for the postscission region as a function of the center of mass distance r of the fragments is given by

$$V(r)=V_c(r)+V_n(r)-V_d(r)-Q,\quad r\geq r_t\ . \tag{1}$$

Here, V_c is the Coulomb potential between a spheroidal daughter nucleus and spherical emitted fragment as in Ref. 8, V_n is the nuclear interaction energy due to finite range effects of Krappe *et al.*,[14] and V_d is the change in the nuclear interaction energy due to quadrupole deformation of the daughter nucleus as in Ref. 14.

The Coulomb potential between the emitted fragments is taken as the interaction of a spheroidal daughter nucleus and a spherical emitted fragment. For a prolate spheroidal daughter nucleus with longer axis along the fission direction, Pik-Pichak[8] obtained

$$V_c(r)=\frac{3}{2}\frac{Z_1Z_2e^2\nu}{r}\left[\frac{1-\nu^2}{2}\ln\frac{\nu+1}{\nu-1}+\nu\right]; \tag{2}$$

and for an oblate spherical daughter nucleus with shorter axis along the fission direction,

$$V_c(r)=\frac{3}{2}\frac{Z_1Z_2e^2}{r}[\nu(1+\nu^2)\arctan\nu^{-1}-\nu^2]\ . \tag{3}$$

Here,

$$\nu=\frac{r}{(a_2^2-b_2^2)^{1/2}}\ , \tag{4}$$

where a_2 and b_2 are the semimajor and minor axes of the spheroidal daughter nucleus, respectively.

For two separated spherical nuclei of equivalent sharp-surface radii R_1 and R_2, the nuclear interaction energy V_n of Krappe *et al.*[14] is given by

$$V_n=-D\left[F+\frac{r-r_{12}}{a}\right]\frac{r_{12}}{r}\exp[(r_{12}-r)/a]\ , \tag{5}$$

where $r_{12}=R_1+R_2$ is the sum of their equivalent sharp-surface radii. Th depth constant D is given by

$$D=\frac{4a^3g(R_1/a)g(R_2/a)e^{-r_{12}/a}C_s'}{r_0^2r_{12}}\ , \tag{6}$$

where

$$g(x)=x\cosh x-\sinh x\ ,$$

and for the case of two separated nuclei,

$$C_s'=[C_s(1)C_s(2)]^{1/2}\ .$$

The constant F is given by

$$F=4+\frac{r_{12}}{a}-\frac{f(R_1/a)}{g(R_1/a)}-\frac{f(R_2/a)}{g(R_2/a)}\ , \tag{7}$$

where

$$f(x)=x^2\sinh x\ ,$$

$$R_i=r_0A_i^{1/3}\ ,$$

$$C_s(i)=a_s(1-K_sI_i^2)\ ,$$

and

$$I_i=(N_i-Z_i)/A_i,\quad (i=1,2)\ . \tag{8}$$

The following values[15] are used for the constants: $r_0=1.16$ fm; $a=0.68$ fm; $a_s=21.13$ MeV, and $K_s=2.3$.

Krappe *et al.*[14] have also derived an expression for the nuclear interaction energy for the case of a spherical nucleus 1 interacting with a deformed nucleus 2 whose nuclear surface is specified in spherical polar coordinates r, θ, and Φ by the equation

$$R(\theta,\Phi)=R_2\left[1+\sum_{n=0}^{\infty}\sum_{m=-n}^{n}\beta_{nm}Y_{nm}(\theta,\Phi)\right]\ ,$$

in a coordinate system located at the center of mass of nucleus 2. In this coordinate system, θ and Φ denote the angular coordinates that specify the location of the center of mass of nucleus 1. Then, the change in the nuclear interaction energy due to the quadrupole deformation β_2' of nucleus 2 is given by

$$V_d=\frac{4R_2^3C_s'A_2'\beta_2'}{ar_0^2}\left[\frac{5}{4\pi}\right]^{1/2}\ , \tag{9}$$

where

$$A_2'=a\frac{\partial}{\partial a}\left\{\left[\frac{R_1}{a}\cosh\left[\frac{R_1}{a}\right]-\sinh\left[\frac{R_1}{a}\right]\right]\left\{\left[\frac{a}{R_2}+3\left[\frac{a}{R_2}\right]^3\right]\sinh\left[\frac{R_2}{a}\right]-3\left[\frac{a}{R_2}\right]^2\cosh\left[\frac{R_2}{a}\right]\right\}\right.$$
$$\left.\times\left[\frac{a}{r}+3\left[\frac{a}{r}\right]^2+3\left[\frac{a}{r}\right]^3\right]e^{-r/a}\right\}. \tag{10}$$

B. Potential for the prescission region

The shape of the barrier in the overlapping region which connects the ground state and the contact point is approximated by a third-order polynomial in r as suggested by Nix[16] having the form

$$V(r)=-E_v+[V(r_t)+E_v]\times\left[s_1\left[\frac{r-r_i}{r_t-r_i}\right]^2-s_2\left[\frac{r-r_i}{r_t-r_i}\right]^3\right],\quad r_i\le r\le r_t\ , \qquad (11)$$

where r_i is the distance between the centers of mass of two portions of the daughter and the emitted nuclei in the spheroidal parent nucleus and

$$r_t=a_2+R_1\ .$$

Here, a_2 is the semimajor or minor axis of the spheroidal daughter nucleus depending on its prolate or oblate shape.

C. Expression for r_i of a deformed parent nucleus

Consider a parent nucleus of spheroidal shape. The radius vector $R(\theta)$ making an angle θ with the axis of maximum deformation locating the effective sharp surface of a deformed nucleus is given by

$$R(\theta)=R_0\left[1+\sum_{n=0}^{\infty}\sum_{m=-n}^{n}\beta_{nm}Y_{nm}(\theta)\right],$$

where R_0 is the radius of equivalent spherical nucleus. If we consider only the spheroidal deformation β_2, then

$$R=R_0[1+\beta_2(5/4\pi)^{1/2}(\tfrac{3}{2}\cos^2\theta-\tfrac{1}{2})]\ . \qquad (12)$$

For a prolate spheroidal parent nucleus with the major axis along the fission direction, the semimajor and minor axes are given by

$$a_0=R_0\left[1+\beta_2\left[\frac{5}{4\pi}\right]^{1/2}\right]$$

and (13)

$$b_0=R_0\left[1-\beta_2\left[\frac{5}{4\pi}\right]^{1/2}\right].$$

Let a planar section cut the parent nucleus into two unequal portions with the masses of the heavy and light nuclei of the decay in question as shown in Fig. 1. The relationship between the heights h_1 and h_2 of the light and heavy portions, respectively, is

$$h_1+h_2=2a_0\ . \qquad (14)$$

If V_1, V_2, and V are the volumes of emitted fragment A_1, daughter nucleus A_2, and parent nucleus A, respectively, then

$$\frac{V_1}{V}=\frac{\pi b_0^2\left[h_1-a_0/3+\frac{(a_0-h_1)^3}{3a_0^2}\right]}{(4/3)\pi a_0 b_0^2}=\frac{A_1}{A}\ .$$

Simplifying, we get

$$3h_1/a_0+(1-h_1/a_0)^3-1=4A_1/A\ . \qquad (15)$$

Solving Eq. (15) numerically and using Eq. (14), one can find the values of h_1 and h_2. The distance r_i between the centers of mass and the two portions in the deformed parent nucleus is now given by the expression

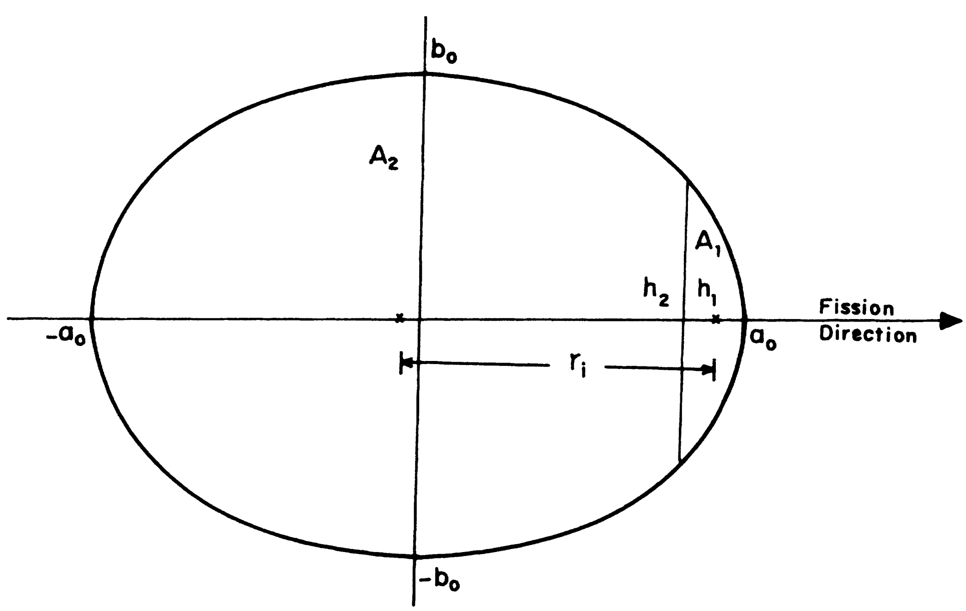

FIG. 1. Prolate spheroidal parent nucleus with a planar section dividing it into two regions with the masses of the daughter and light nuclei.

$$r_i=\frac{3}{4}\left[\frac{h_1^2}{a_0+h_1}+\frac{h_2^2}{a_0+h_2}\right]. \tag{16}$$

If the Nilsson's hexadecapole deformation parameter β_4 is also included in the parent deformation, then Eq. (12) becomes

$$R=R_0[1+\beta_2(5/4\pi)^{1/2}(\tfrac{3}{2}\cos^2\theta-\tfrac{1}{2}) +\beta_4(9/4\pi)^{1/2}\tfrac{1}{8}(35\cos^4\theta-30\cos^2\theta+3)]\ ; \tag{17}$$

and Eq. (13) becomes

$$a_0=R_0\left[1+\left[\frac{5}{4\pi}\right]^{1/2}\beta_2+\left[\frac{9}{4\pi}\right]^{1/2}\beta_4\right]. \tag{18}$$

The values of r_i calculated for the parent nucleus treating it as sphere, including spheroidal deformation β_2 only and also adding Nilsson's hexadecapole deformation β_4 (both β_2 and β_4 are taken from Ref. 17), are presented in Table I.

D. Q value of the reaction

If Q is the energy released in the reaction, its value is given by

$$Q=[M(Z,A)-M(Z_1,A_1)-M(Z_2,A_2)] \times 931.501\ \text{MeV}. \tag{19}$$

Q values for different decay modes are calculated using the mass table of Wapstra and Audi[18] and used so as to incorporate the shell effects at the ground states.

E. Inclusion of zero-point vibration energy

While including the zero-point vibration energy E_v in the calculation of the lifetimes, one has to be careful to see that the conservation of energy is preserved. In order to accomplish this, we follow the consistent procedure to fit the cubic part of the barrier not to zero at $r=r_t$ but to $-E_v$. For E_v, we choose[9]

$$E_v=\frac{\pi\hbar}{2}\frac{(2Q/\mu)^{1/2}}{(C_1+C_2)}, \tag{20}$$

where C_1 and C_2 are the "central" radii of the fragments given by[19]

$$C_i=1.18A_i^{1/3}-0.48\quad(i=1,2), \tag{21}$$

and μ is the reduced mass of the system.

F. Nuclear inertial mass coefficient

The nuclear inertial mass coefficient $B_r(r)$ is taken to be deformation dependent and the expression for the inertia of the new valley in the semiempirical model of Moller *et al.*[20] is

$$B_r(r)-\mu=f(r,r_t)k(B_r^{irr}-\mu), \tag{22}$$

where

$$k=16\ ;$$

$$r_t=a_2+R_1\ ;$$

and

$$f(r,r_t)=\begin{cases}[(r_t-r)/(r_t-r_i)]^4, & r\le r_t\ ,\\ 0, & r\le r_t\ .\end{cases} \tag{23}$$

Here, B_r^{irr} is the inertia corresponding to hydrodynamical flow whose numerical results are approximated by Moller and Nix[21] as

$$B_r^{irr}-\mu=\tfrac{17}{15}\mu\exp[-\tfrac{128}{51}(r-\tfrac{3}{4})]$$

for the case of symmetric fission (r is expressed here in terms of R_0). For exotic decay studies, we use

$$B_r^{irr}-\mu=\tfrac{17}{15}\mu\exp\left[-\frac{128}{51}\left[\frac{r-r_i}{a_0}\right]\right], \tag{24}$$

where a_0 is the semimajor axis of the prolate spheroidal parent.

TABLE I. The effect of ground-state deformations of the parent nucleus on the r_t values.

S. no.	Parent nucleus	Emitted nucleus	Ground-state deformations of parent, Ref. 17 β_2	β_4	r_t (fm) treating the parent nucleus as Sphere	β_2 only	β_2 and β_4
1	^{221}Fr	^{14}C	0.098	−0.060	5.9783	6.3479	6.0443
2	^{221}Ra	^{14}C	0.098	−0.060	5.9783	6.3479	6.0443
3	^{222}Ra	^{14}C	0.104	−0.060	5.9890	6.3819	6.0778
4	^{223}Ra	^{14}C	0.138	−0.075	5.9997	6.5220	6.1412
5	^{224}Ra	^{14}C	0.144	−0.075	6.0104	6.5563	6.1749
6	^{225}Ac	^{14}C	0.151	−0.080	6.0210	6.5945	6.1869
7	^{226}Ra	^{14}C	0.151	−0.080	6.0317	6.6062	6.1978
8	^{231}Pa	^{24}Ne	0.185	−0.080	5.8665	6.5511	6.1539
9	^{232}U	^{24}Ne	0.192	−0.080	5.8768	6.5885	6.1906
10	^{233}U	^{24}Ne	0.192	−0.080	5.8870	6.6000	6.2014
11	^{234}U	^{26}Ne	0.198	−0.075	5.8635	6.5968	6.2236
12	^{234}U	^{28}Mg	0.198	−0.075	5.8320	6.5604	6.1903
13	^{237}Np	^{30}Mg	0.198	−0.070	5.8328	6.5613	6.2158
14	^{241}Am	^{34}Si	0.212	−0.050	5.8188	6.5970	6.3508

TABLE II. Comparison of calculated values of $\log_{10}(T/T_\alpha)$ of ^{14}C and ^{24}Ne emissions without deformation (a), with spheroidal deformation β_2' in daughter only (b), and with spheroidal β_2 and hexadecapole β_4 deformations in parent and spheroidal deformation in daughter nuclei (c) with experimental values.

S. no.	Decay mode	Deformations, Ref. 17 Parent β_2	β_4	Daughter β_2'	$\log_{10}(T/T_\alpha)$ This work a	b	c	Experimental Ref. 24
1	$^{221}Fr \to ^{207}Ti + ^{14}C$	0.098	−0.060	0.003	12.13	12.04	12.05	> 13.3
2	$^{221}Ra \to ^{207}Pb + ^{14}C$	0.098	−0.060	0.003	11.86	11.87	11.79	> 12.9
3	$^{222}Ra \to ^{208}Pb + ^{14}C$	0.104	−0.060	0.003	10.34	10.35	10.24	9.43±0.06
4	$^{223}Ra \to ^{209}Pb + ^{14}C$	0.138	−0.075	0.003	8.39	8.40	8.21	9.21±0.05
5	$^{224}Ra \to ^{210}Pb + ^{14}C$	0.144	−0.075	0.003	11.74	11.75	11.52	10.37±0.12
6	$^{225}Ac \to ^{211}Bi + ^{14}C$	0.151	−0.080	0.003	12.55	12.56	12.31	> 12.4
7	$^{226}Ra \to ^{212}Pb + ^{14}C$	0.151	−0.080	0.003	12.03	12.04	11.77	10.6±0.2
8	$^{230}Th \to ^{206}Hg + ^{24}Ne$	0.185	−0.075	−0.003	14.31	14.30	12.85	12.25±0.07
9	$^{231}pa \to ^{207}Tl + ^{24}Ne$	0.185	−0.080	0.003	10.93	10.95	10.32	11.22
10	$^{232}U \to ^{208}Pb + ^{24}Ne$	0.192	−0.080	0.003	11.90	11.92	11.25	11.7±0.1
11	$^{233}U \to ^{209}Pb + ^{24}Ne$	0.192	−0.080	0.003	11.62	11.65	10.93	12.12±0.15
12	$^{234}U \to ^{210}Pb + ^{24}Ne$	0.198	−0.075	0.003	14.36	14.39	13.49	12.48±0.07

G. Evaluation of constants s_1 and s_2

The constants s_1 and s_2 appearing in Eq. (11) are determined by requiring that the value of the potential $V(r)$ and its first derivative be continuous at the contact point $r = r_t$. Thus, we get

$$s_1 = 3 - S ;$$

and

$$s_2 = 2 - S ;$$

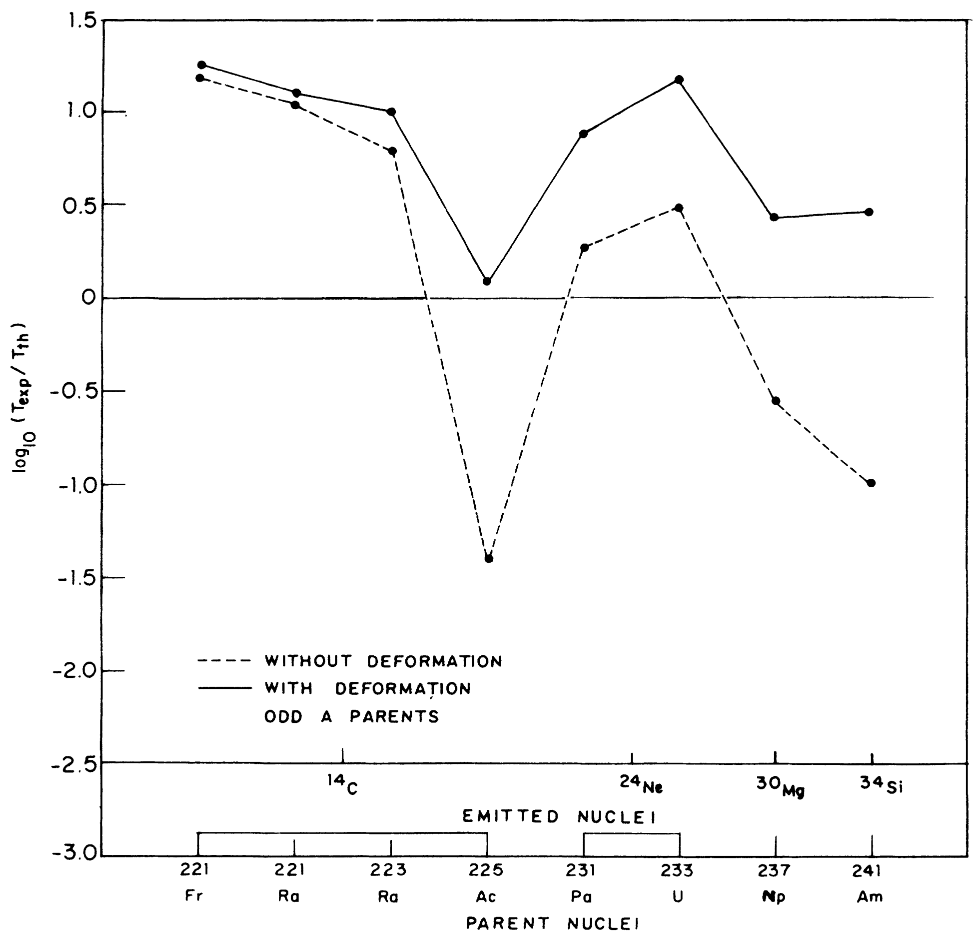

FIG. 2. The effect of deformations on $\log_{10}(T/T_\alpha)$ for odd A parent nuclei.

TABLE III. Comparison of calculated values of $\log_{10}(T/T_\alpha)$ of ^{26}Ne, ^{28,30}Mg, and ^{34}Si emissions without deformation (a), and with spheroidal β_2 and hexadecapole β_4 deformations in parent and spheroidal deformation β_2' in daughter nuclei (b) with experimental values.

S		Deformations, Ref. 17			$\log_{10}(T/T_\alpha)$		
		Parent		Daughter	This work		Experimental
no.	Decay mode	β_2	β_4	β_2'	a	b	Ref. 24
1	$^{232}Th \rightarrow ^{206}Hg + ^{26}Ne$	0.192	−0.070	−0.003	12.66	11.79	> 10.3
2	$^{234}U \rightarrow ^{208}Pb + ^{26}Ne$	0.198	−0.075	0.003	14.39	13.58	12.48±0.07
3	$^{234}U \rightarrow ^{206}Hg + ^{28}Mg$	0.198	−0.075	−0.003	13.76	12.85	12.82±0.11
4	$^{238}Pu \rightarrow ^{210}Pb + ^{28}Mg$	0.205	−0.060	0.003	17.26	15.98	
5	$^{237}Np \rightarrow ^{207}Tl + ^{30}Mg$	0.198	−0.070	0.003	13.94	12.95	> 13.4
6	$^{238}Pu \rightarrow ^{208}Pb + ^{30}Mg$	0.205	−0.060	0.003	17.53	16.27	
7	$^{238}Pu \rightarrow ^{206}Hg + ^{32}Si$	0.205	−0.060	−0.003	17.39	16.03	
8	$^{241}Am \rightarrow ^{207}Tl + ^{34}Si$	0.212	−0.050	0.003	15.07	13.63	> 15.1; > 14.1

where

$$S=\frac{r_t-r_i}{[V(r_t)+E_v]}[V_c'(r_t)+V_n'(r_t)-V_d'(r_t)] . \quad (25)$$

H. Lifetime calculation

Expressing the energies in MeV, lengths in fm, and time in seconds, for calculating the lifetime of the decay system we use the formula[22]

$$T=\frac{1.433\times 10^{-21}}{E_v}[1+\exp K] . \quad (26)$$

The action integral K is given by

$$K=\frac{2}{\hbar}\left\{\int_{r_a}^{r_t}[2B_r(r)V(r)]^{1/2}dr + \int_{r_t}^{r_b}[2B_r(r)V(r)]^{1/2}dr\right\} . \quad (27)$$

The limits of integration r_a and r_b are the two appropriate zeros of the integrand which are found numerically.

III. RESULTS AND DISCUSSION

The present model is applied first to calculate the lifetimes T for the spontaneous emission of ^{14}C and ^{24}Ne

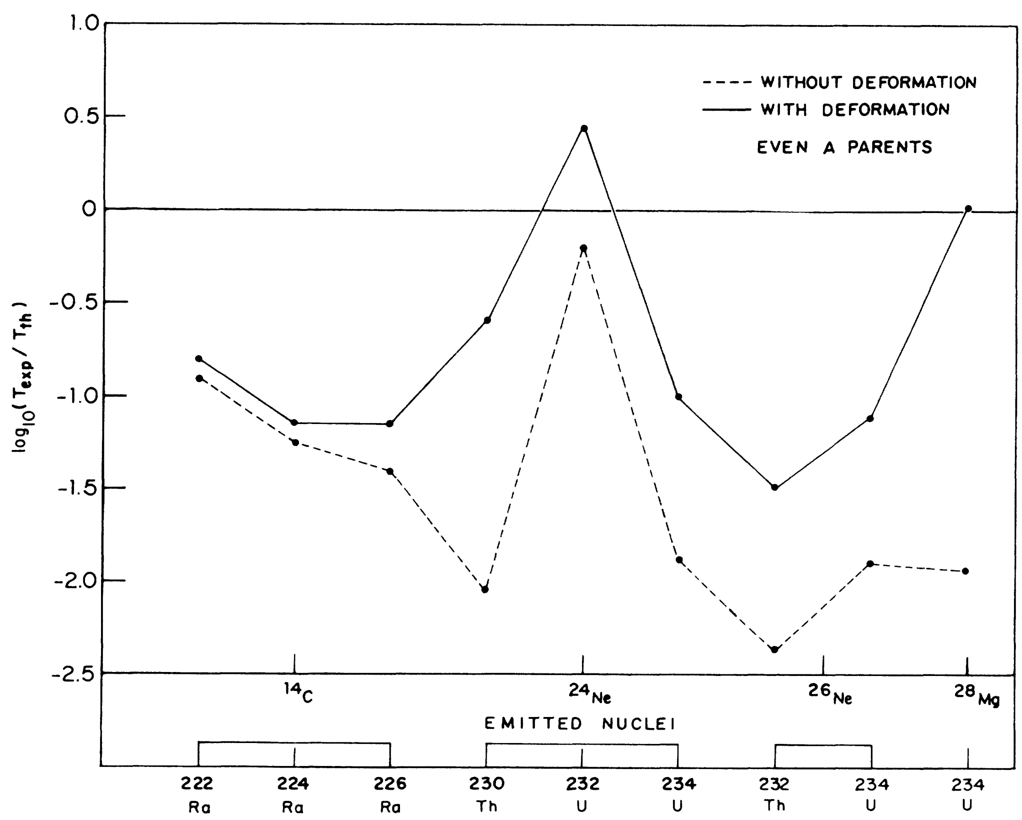

FIG. 3. Same as in Fig. 2 for even A parent nuclei.

treating both the parent and the emitted nuclei as spheres and including only the quadrupole deformation in the daughter nucleus. The branching ratios are then obtained by using the experimental half-lives[23] of the respective alpha disintegration (T_α). Since the deformations involved here are rather very small, their effect on lifetimes is not all appreciable. But, when the ground-state spheroidal and hexadecapole deformations are included in the parent nuclei, the lifetimes and hence the branching ratios are affected appreciably (see Table II). In studying the emissions of ^{26}Ne, ^{28,30}Mg, and ^{34}Si, we have thus introduced the deformations both in the parent and the daughter nuclei keeping the emitted nucleus spherical. The results obtained are compared with the experimental values[24] in Table III.

We find from Tables II and III that the branching ratios of exotic decays are lowered due to inclusion of deformations. The ground-state deformations of the parent nucleus enhances the r_i value in these decay modes and hence the barrier to be penetrated is very much narrowed.

The effects of deformation for odd and even A parent nuclei are plotted in Figs. 2 and 3. It is noticed that in the case of the even A parent nucleus, the deformation brings the theoretical values closer to the experimental ones whereas in the case of the odd A parent nucleus, the theoretical results are slightly disturbed.

To summarize, in this work, we have extended our previous model for exotic decay studies by incorporating the deformation of the parent and daughter nuclei in the calculations. In the postscission region this inclusion alters the Coulomb as well as the nuclear surface energy due to finite range effects while in the prescission region, the values of r_i and r_t are getting modified. While the deformation of the parent nuclei affects the results much, the deformation of the daughter nuclei being very small hardly affects the results. Thus, it seems that in almost all the exotic decays reported so far, the daughter and the emitted fragments always prefer to be spherical which may be due to the consequence of the shell effects.

[1]A. Sandulescu, D. M. Poenaru, and W. Greiner, Fiz. Elem. Chastits At. Yadra **11**, 1334 (1980) [Sov. J. Part. Nucl. **11**, 528 (1980)].

[2]H. J. Rose and G. A. Jones, Nature (London) **307**, 245 (1984).

[3]S. Gales, E. Hourani, M. Hussonnois, J. P. Schapira, L. Stab, and M. Vergnes, Phys. Rev. Lett. **53**, 759 (1984).

[4]P. B. Price, J. D. Stevenson, S. W. Barwick, and H. L. Ravn, Phys. Rev. Lett. **54**, 297 (1985).

[5]S. Wang, P. B. Price, S. W. Barwick, K. J. Moody, and E. K. Hulet, Phys. Rev. C **36**, 2717 (1987); S. P. Tretyakova, A. Sandulescu, V. L. Micheev, D. Hasegan, I. A. Lededev, Yu. S. Zamyatnin, Yu. S. Korotkin, and B. F. Myasoedov, Joint Institute for Nuclear Research Report No. 13-85, 1985; K. J. Moody, E. K. Hulet, S. Wang, P. B. Price, and S. W. Barwick, Phys. Rev. C **36**, 2710 (1987).

[6]D. N. Poenaru and M. Ivascu, J. Phys. (Paris) **45**, 1099 (1984).

[7]Y. J. Shi and W. J. Swiatecki, Phys. Rev. Lett. **54**, 300 (1985); Nucl. Phys. **A438**, 450 (1985).

[8]G. A. Pik-Pichak, Yad. Fiz. **44**, 1421 (1986) [Sov. J. Nucl. Phys. **44**, 923 (1986)].

[9]H. G. de Carvalho, J. B. Martins, and O. A. P. Tavares, Phys. Rev. C **34**, 2261 (1986).

[10]R. Blendowske and H. Walliser, Phys. Rev. Lett. **61**, 1930 (1988).

[11]G. Shanmugam and B. Kamalaharan, Phys. Rev. C **38**, 1377 (1988).

[12]G. Shanmugam and B. Kamalaharan, in *Proceedings of the International Conference on Nuclear Reaction Mechanism at Calcutta, India, 1989,* edited by S. Mukherjee (Sinp and Vecc, Calcutta, 1989), p. 73.

[13]Y. J. Shi and W. J. Swiatecki, Nucl. Phys. **A464**, 205 (1987).

[14]H. J. Krappe, J. R. Nix, and A. J. Sierk, Phys. Rev. C **20**, 992 (1979).

[15]P. Moller and J. R. Nix, Nucl. Phys. **A361**, 117 (1981).

[16]J. R. Nix, Ann. Phys. (N.Y.) **41**, 52 (1967).

[17]P. Moller and J. R. Nix, At. Data Nucl. Data Tables **26**, 165 (1981).

[18]A. H. Wapstra and G. Audi, Nucl. Phys. **A432**, 1 (1985).

[19]R. Hofstadeter, in *Nuclear Radii,* Vol. 2 of *Nuclear Physics and Technology,* edited by H. Schopper (Springer-Verlag, Berlin, 1967).

[20]P. Moller, J. R. Nix, and W. J. Swiatecki, Nucl. Phys. **A469**, 1 (1987).

[21]P. Moller and J. R. Nix, Phys. Rev. Lett. **37**, 1461 (1976).

[22]D. N. Poenaru and M. Ivascu, J. Phys. **45**, 1099 (1984).

[23]A. Rytz, At. Data Nucl. Data Tables **12**, 4791 (1973).

[24]P. B. Price (private communication).